JCI insight

RESEARCH ARTICLE

Inhibition of stromal cell–derived factor-1α/CXCR4 signaling restores the blood-retina barrier in pericyte-deficient mouse retinas

Keisuke Omori,[1] Nanae Nagata,[1] Kaori Kurata,[2] Yoko Fukushima,[3] Erika Sekihachi,[1] Nobutaka Fujii,[4] Tomoko Namba-Hamano,[5] Yoshitsugu Takabatake,[5] Marcus Fruttiger,[6] Takashi Nagasawa,[7] Akiyoshi Uemura,[2] and Takahisa Murata[1]

[1]Department of Animal Radiology, Graduate School of Agriculture and Life Sciences, The University of Tokyo, Tokyo, Japan. [2]Department of Retinal Vascular Biology, Nagoya City University Graduate School of Medical Sciences, Nagoya, Japan. [3]Department of Ophthalmology, Graduate School of Medicine, Osaka University, Osaka, Japan. [4]Laboratory of Bioorganic Medicinal Chemistry and Chemogenomics, Graduate School of Pharmaceutical Sciences, Kyoto University, Kyoto, Japan. [5]Department of Nephrology, Graduate School of Medicine, Osaka University, Osaka, Japan. [6]UCL Institute of Ophthalmology, University College London, London, United Kingdom. [7]Laboratory of Stem Cell Biology and Developmental Immunology, Graduate School of Frontier Biosciences and Graduate School of Medicine, Osaka University, Osaka, Japan.

In diabetic retinopathy (DR), pericyte dropout from capillary walls is believed to cause the breakdown of the blood-retina barrier (BRB), which subsequently leads to vision-threatening retinal edema. While various proinflammatory cytokines and chemokines are upregulated in eyes with DR, their distinct contributions to disease progression remain elusive. Here, we evaluated roles of stromal cell–derived factor-1α (SDF-1α) and its receptor CXCR4 in the BRB breakdown initiated by pericyte deficiency. After inhibition of pericyte recruitment to developing retinal vessels in neonatal mice, endothelial cells (ECs) upregulated the expression of SDF-1α. Administration of CXCR4 antagonists, or EC-specific disruption of the CXCR4 gene, similarly restored the BRB integrity, even in the absence of pericyte coverage. Furthermore, CXCR4 inhibition significantly decreased both the expression levels of proinflammatory genes ($P < 0.05$) and the infiltration of macrophages ($P < 0.05$) into pericyte-deficient retinas. Taken together, EC-derived SDF-1α induced by pericyte deficiency exacerbated inflammation through CXCR4 in an autocrine or paracrine manner and thereby induced macrophage infiltration and BRB breakdown. These findings suggest that the SDF-1α/CXCR4 signaling pathway may be a potential therapeutic target in DR.

Introduction

Diabetic retinopathy (DR) is a leading cause of vision loss in working-age populations. DR occurs in about 35% of diabetic patients, with most of its symptoms being ascribable to anatomical and functional abnormalities in retinal blood vessels (1). For instance, diabetic macular edema (DME) resulting from blood-retina barrier (BRB) breakdown and subsequent vascular hyperpermeability may impair central vision at any clinical stage of DR (2). Since protein concentration of VEGF is increased in eyes with DR (3), intravitreal injections of anti-VEGF drugs have been globally employed for the treatment of DME. While anti-VEGF drugs are beneficial for vision maintenance and improvement in DR patients, repeated injections are usually required owing to DME recurrence (4). Moreover, a considerable proportion of patients are refractory to anti-VEGF drugs, suggesting the presence of a VEGF-independent signaling pathway being involved in at least some DME cases (5).

Various proinflammatory cytokines and chemokines are also upregulated in eyes with DR (6, 7). Among them is stromal cell–derived factor-1α (SDF-1α), also known as CXCL12. Intravitreal levels of SDF-1α are intimately correlated with the presence of DME (8). SDF-1α binds to G protein–coupled CXCR4, which is expressed in endothelial cells (ECs), immune cells, hematopoietic stem cells, and neurons (9–12). Pharmacologic and genetic manipulation studies demonstrate critical roles for SDF-1α/CXCR4 signaling in retinal

Conflict of interest: The authors have declared that no conflict of interest exists.

Submitted: February 26, 2018
Accepted: October 31, 2018
Published: December 6, 2018

Reference information:
JCI Insight. 2018;3(23):e120706.
https://doi.org/10.1172/jci.insight.120706.

angiogenic processes, including vascular sprouting and artery formation (13). We previously reported the direct effects of endothelial SDF-1α/CXCR4 signaling on the modulation of vascular permeability and inflammation (14). However, specific roles of this signaling axis in the initiation and progression of DR remain elusive, primarily because hyperglycemic animal models fail to fully reproduce the pathophysiology of DR.

Histological analyses of human retinas imply that dropout of pericytes from retinal capillary walls leads to BRB breakdown in DR (15). Consistent with this notion, pericyte depletion in developing mouse retinas through disruption of PDGF/PDGFRβ signaling produces clinical features of DR, such as retinal vascular tortuosity and dilation and retinal edema and hemorrhage (16–19). Notably, in developing retinal vessels, pericyte deficiency directly induces inflammatory responses in ECs and subsequent infiltration of macrophages (20). The infiltrating macrophages further inflame ECs by secreting propermeable and proinflammatory cytokines, including VEGF. This vessel-damaging loop between ECs and macrophages leads to irreversible BRB breakdown (20). Therefore, signaling molecules involved in EC-macrophage interactions in pericyte-deficient retinas may be potential novel targets to treat DR.

In the current study, we identified SDF-1α/CXCR4 signaling as a crucial exacerbating factor in the inflammatory loop between ECs and macrophages in BRB breakdown following pericyte deficiency. Our findings support the conclusion that blocking the SDF-1α/CXCR4 signaling pathway may have clinical implications in the management of DR.

Results

Pericyte deficiency induced BRB breakdown that mimicked DR pathology. In mock-treated C57/BL6 P8 mice, nearly the entire retinal surface was covered by vessels composed of isolectin B4–positive ECs (Supplemental Figure 1A, top left; supplemental material available online with this article; https://doi.org/10.1172/jci.insight.120706DS1). The ECs were enveloped by desmin-positive pericytes at both the vascular front and plexus (Supplemental Figure 1A, bottom left).

As previously shown (20), single intraperitoneal injections of anti-PDGFRβ antibody APB5 resulted in distorted, shortened, and dilated retinal vessels in P8 mice (Supplemental Figure 1A, top right, and Supplemental Figure 1B). The treatment almost completely inhibited the recruitment of pericytes to the retinal vessels (Supplemental Figure 1A, bottom right). The APB5-induced pericyte deficiency increased the leakage of the plasma-component fibrinogen outside the retinal vessels, indicating a BRB breakdown (Supplemental Figure 1C). In addition, F4/80-positive round-shaped macrophages were infiltrated in the APB5-treated retina (Supplemental Figure 1D).

SDF-1α expression increased in pericyte-deficient retinas. We evaluated *Sdf1a* mRNA expression in murine retinas. A previous report demonstrated that APB5-induced pericyte deficiency induced inflammatory responses in ECs of retinal vessels in P5 mice and caused severe edema and hemorrhage in P10 retinas (20). Consistent with this, our treatment of mice with APB5 significantly increased the *Sdf1a* retinal expression in P5, P7, and P9 mice (Figure 1A).

In situ hybridization of P8 mouse retinas revealed broadly expressed *Sdf1a* in mock-treated animals, including collagen IV–positive ECs (Figure 1B, left, shown by white arrowheads). In APB5-treated mice, retinal *Sdf1a* expression in ECs was markedly increased (Figure 1B, right, shown by white arrowheads).

CXCR4 expressed in the endothelium of pericyte-deficient retina. Previous reports showed that the SDF-1α receptor CXCR4 is expressed in endothelial tip cells and arterial ECs in retinas of postnatal mice (13). Consistent with this report, flow cytometry analysis showed that 66% of $CD31^+CD45^-$ ECs expressed CXCR4 in mock-treated mice (Figure 1D). Treatment with APB5 resulted in $CD11b^+CD45^{hi}$ macrophages (20) infiltrating the P8 retinas (Figure 1C). In retinas of APB5-treated mice, approximately 80% of $CD31^+CD45^-$ ECs expressed CXCR4 (Figure 1D), compared with about 8% of the macrophages (Figure 1C). In line with these results, in situ hybridization of *Cxcr4* in P8 mouse retinas revealed that *Cxcr4* was mainly localized to collagen IV–positive ECs both in PBS- and APB5-treated mouse retinas (Supplemental Figure 2, shown by white arrowheads).

Endothelial CXCR4 deficiency ameliorated the BRB disruption. We evaluated the functional contribution of endothelial CXCR4 using tamoxifen-inducible endothelial-specific CXCR4-deficient mice ($CXCR4^{i\Delta EC}$). Retinas from noninduced Cre^- and induced Cre^+ mice were analyzed at P8. In mock-treated mice, endothelial CXCR4 deficiency did not affect vascular/BRB formation and macrophage infiltration (Figure 2). APB5 treatment shortened, dilated, and distorted the retinal vessels of the Cre^- mice exhibiting a wild-type CXCR4 phenotype (Figure 2, A and B). It also disrupted the BRB (Figure 2, C and D) and resulted in

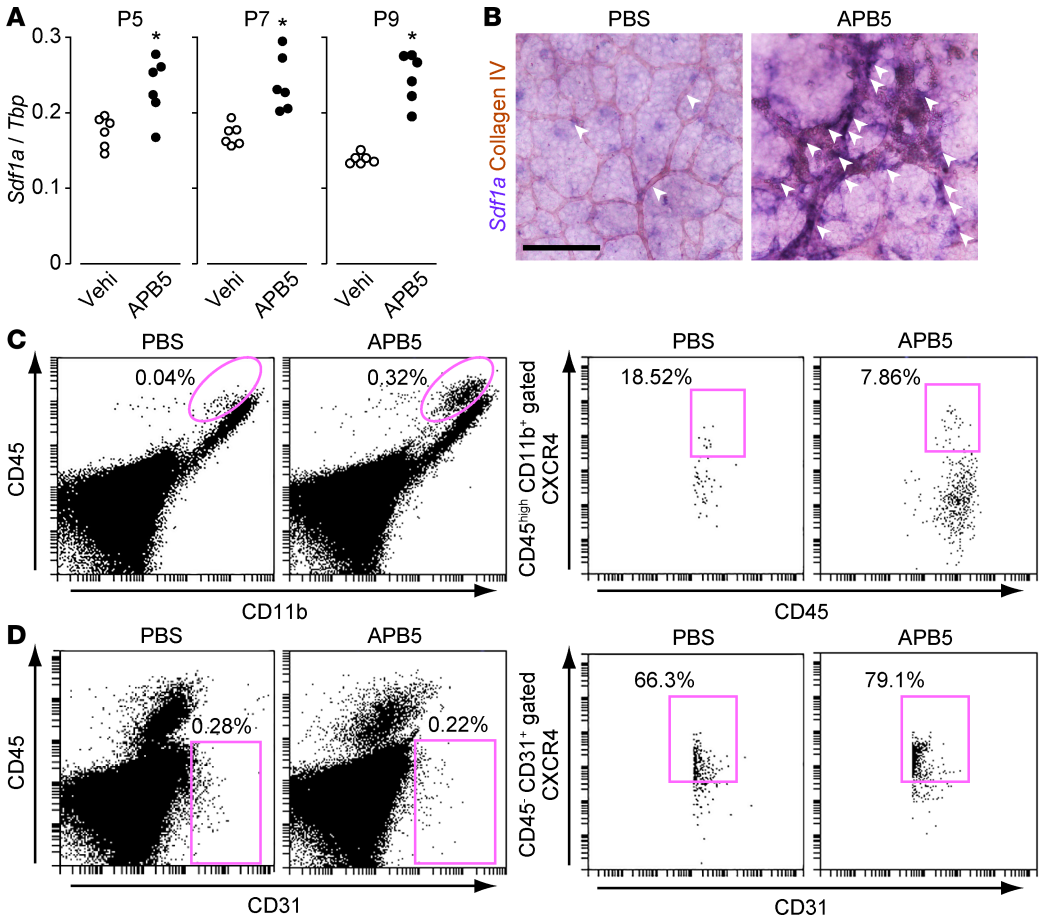

Figure 1. SDF-1α/CXCR4 expression was observed in retinal ECs in APB5-treated mouse retina. (**A**) The effect of APB5 on *Sdf1a* mRNA expression in P5, P7, and P9 mouse retinas ($n = 6$). (**B**) Representative images of retina in situ hybridization of *Sdf1a* (purple) and collagen IV (brown) on P8. White arrowheads indicate a double-positive staining region of *Sdf1a* and collagen IV. Scale bar: 50 μm. (**C**) Representative images of P8 mouse flow cytometry. Pink circles in left 2 graphs indicate $CD11b^+CD45^{hi}$ macrophages. Pink rectangles in right 2 graphs indicate CXCR4-positive macrophages. (**D**) Representative images of P8 mouse flow cytometry. Pink rectangles in left 2 graphs indicate $CD31^+CD45^-$ ECs. Pink rectangles in 2 right graphs indicate CXCR4-positive ECs. Significantly different from the results in vehicle-treated mice at $^*P < 0.05$, significantly different from the results in vehicle-treated mice.

elevated macrophage infiltration into the retina (Figure 2, E and F). APB5 treatment of induced Cre^+ mice that had an endothelial-specific CXCR4-deficient phenotype and caused extension, narrowing, and retention of the retinal vessels (Figure 2, A and B). Induced CXCR4 deficiency also significantly attenuated BRB breakdown (Figure 2, C and D) and macrophage infiltration (Figure 2, E and F).

CXCR4 inhibition abrogated the pericyte deficiency–induced BRB disruption. We assessed whether pharmacological inhibition of SDF-1α/CXCR4 signaling was beneficial against pericyte deficiency–induced BRB disruption. As shown in Figure 3, A and B, treatment of mice with CXCR4 inhibitor AMD3100 or FC131 on P3, P5, and P7 ameliorated the APB5-induced vascular shortening (almost complete inhibition) and dilation (about 60% inhibition). These inhibitors also significantly protected the mice from BRB disruption (Figure 3, C and D; about 40% inhibition) and macrophage infiltration (Figure 3, E and F; about 65% inhibition).

In consideration and comparison of potential therapeutic application, we intravitreally administrated AMD3100 (P5; 1 μg/eye) and/or VEGF Trap (current first-line drug against DR, P5; 2.5 μg/eye). Local treatment with AMD3100 showed beneficial effect against APB5-induced BRB breakdown, which was comparable to VEGF Trap (Figure 4, A–E). However, we could not observe a synergistic effect of AMD3100 and VEGF Trap in these protocols (Figure 4, A–E).

We further evaluated the effect of pharmacological blocking of CXCR4 on the advanced forms of pericyte depletion–induced BRB breakdown. As shown in the middle image of Figure 4F, APB5 treatment

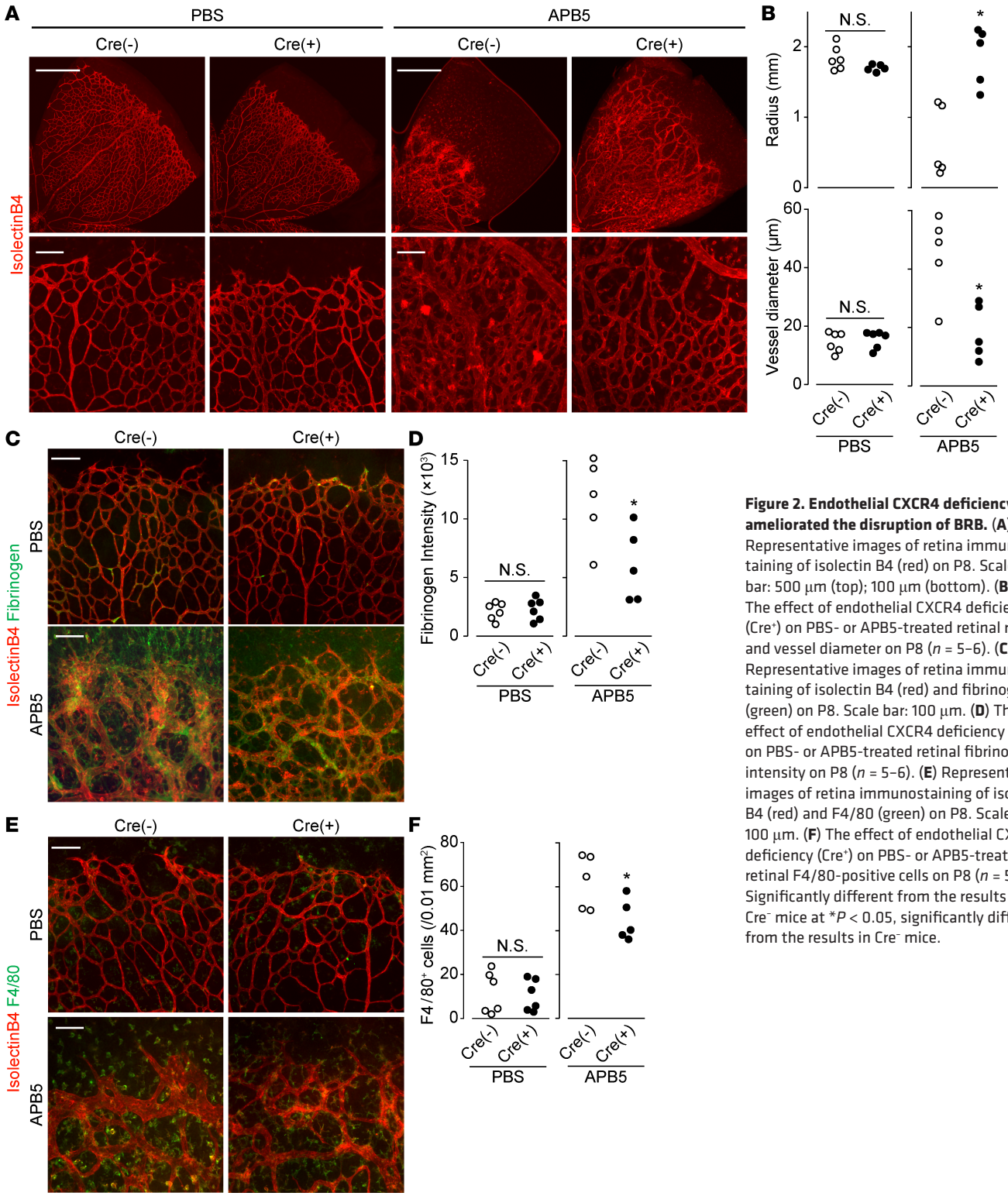

Figure 2. Endothelial CXCR4 deficiency ameliorated the disruption of BRB. (**A**) Representative images of retina immunostaining of isolectin B4 (red) on P8. Scale bar: 500 μm (top); 100 μm (bottom). (**B**) The effect of endothelial CXCR4 deficiency (Cre⁺) on PBS- or APB5-treated retinal radius and vessel diameter on P8 (n = 5–6). (**C**) Representative images of retina immunostaining of isolectin B4 (red) and fibrinogen (green) on P8. Scale bar: 100 μm. (**D**) The effect of endothelial CXCR4 deficiency (Cre⁺) on PBS- or APB5-treated retinal fibrinogen intensity on P8 (n = 5–6). (**E**) Representative images of retina immunostaining of isolectin B4 (red) and F4/80 (green) on P8. Scale bar: 100 μm. (**F**) The effect of endothelial CXCR4 deficiency (Cre⁺) on PBS- or APB5-treated retinal F4/80-positive cells on P8 (n = 5–6). Significantly different from the results in Cre⁻ mice at $^*P < 0.05$, significantly different from the results in Cre⁻ mice.

induced severe edema and hemorrhage, resulting in retinal collapse. Intraperitoneal AMD3100 treatment once daily from P8 through P10 significantly attenuated both the edema and hemorrhaging (Figure 4, F and G), suggesting therapeutic potential for pharmaceutical blocking of CXCR4.

Inhibition of CXCR4 decreased CCL2, ICAM-1, and E selectin mRNA expression. Macrophage infiltration is both a causative and an exacerbating factor of BRB breakdown in the absence of pericytes (20). Consistently, depletion of macrophages by clodronate liposome (7 mg/ml, i.p., P4 and P5) in APB5-treated mouse

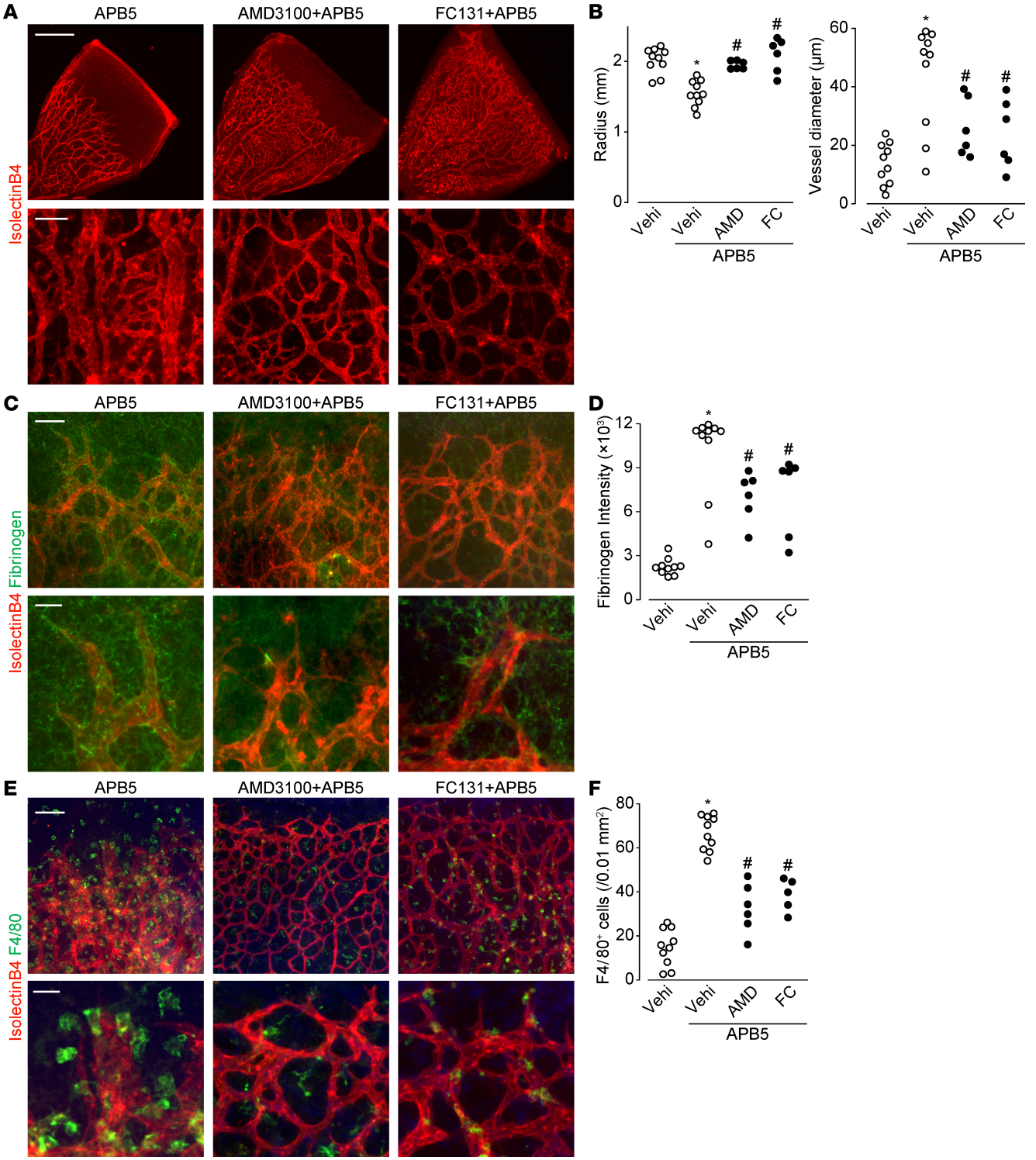

Figure 3. CXCR4 inhibition abrogated the progression of APB5-induced BRB breakdown and macrophage infiltration. (**A**) Representative images of retina immunostaining of isolectin B4 (red) on P8. Scale bar: 500 μm (top); 50 μm (bottom). (**B**) The effect of AMD3100 (AMD) or FC131 (FC) on APB5-treated retinal radius and vessel diameter on P8 (n = 6–10). (**C**) Representative images of retina immunostaining of isolectin B4 (red) and fibrinogen (green) on P8. Scale bar: 100 μm (top); 30 μm (bottom). (**D**) The effect of AMD3100 or FC131 on APB5-treated retinal fibrinogen intensity on P8 (n = 6–10). (**E**) Representative images of retina immunostaining of isolectin B4 (red) and F4/80 (green) on P8. Scale bar: 100 μm (top); 30 μm (bottom). (**F**) The effect of AMD3100 or FC131 on APB5-treated retinal F4/80-positive cells on P8 (n = 6–10). Significantly different from the results in PBS- or APB5-treated mice at $^{*}P < 0.05$, significantly different from the results in PBS-treated mice. $^{\#}P < 0.05$, significantly different from the results in APB5-treated mice.

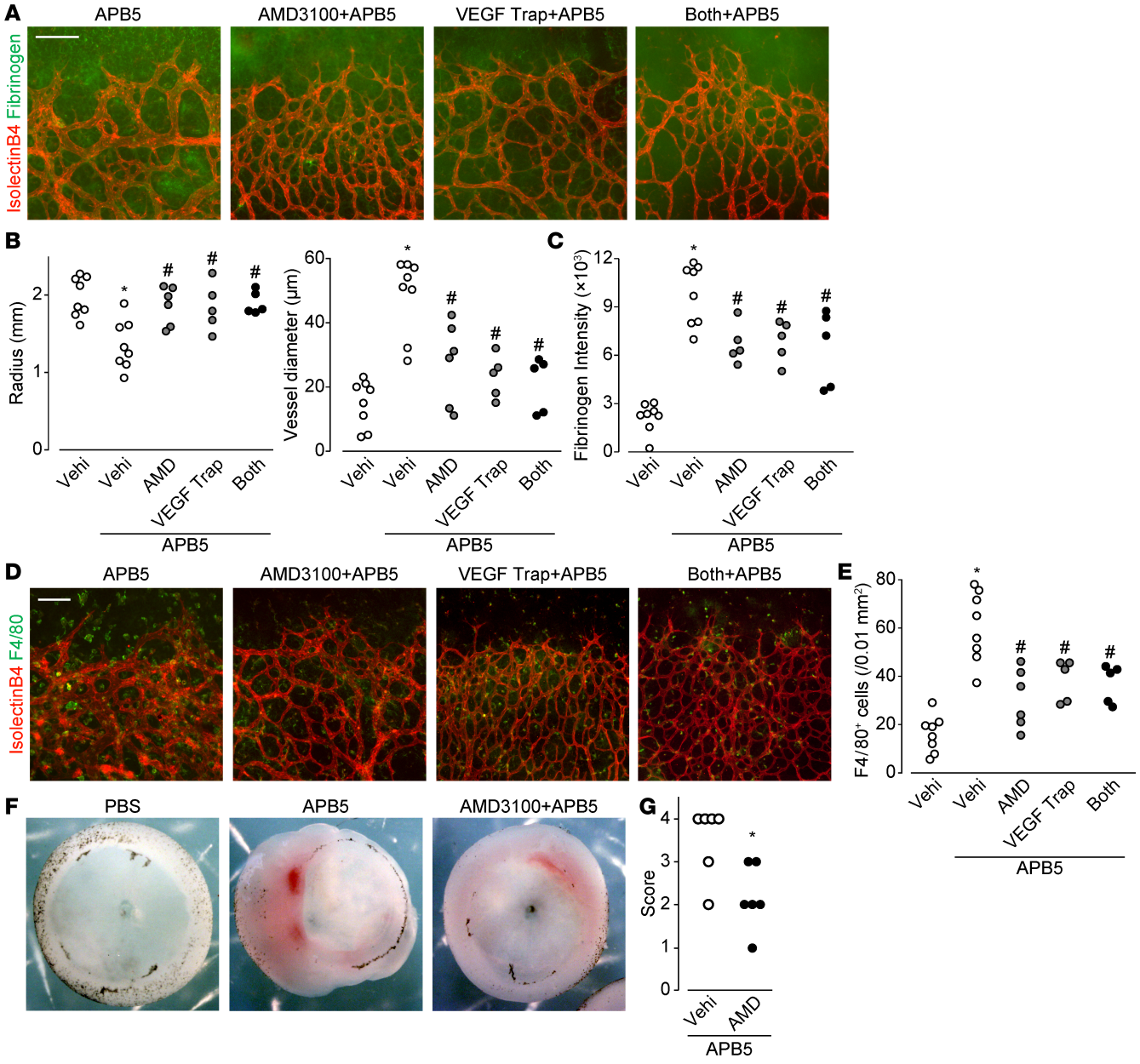

Figure 4. Local CXCR4 inhibition abrogated the APB5-induced pathologies comparably to VEGF Trap. (**A**) Representative images of retina immunostaining of isolectin B4 (red) and fibrinogen (green) on P8. Scale bar: 100 μm. (**B**) The effect of AMD3100 (AMD) and/or VEGF Trap on APB5-treated retinal radius and vessel diameter on P8 (n = 5–8). (**C**) The effect of AMD3100 and/or VEGF Trap on APB5-treated retinal fibrinogen intensity on P8 (n = 5–8). (**D**) Representative images of retina immunostaining of isolectin B4 (red) and F4/80 (green) on P8. Scale bar: 100 μm. (**E**) The effect of AMD3100 and/or VEGF Trap on APB5-treated retinal F4/80-positive cells on P8 (n = 5–8). (**F**) Representative images of P11 mouse retina. (**G**) Retina grading scores of APB5- or APB5 and AMD3100–treated P11 mice (n = 6). Significantly different from the results in PBS- or APB5-treated mice at $^{*}P < 0.05$, significantly different from the results in PBS-treated mice. $^{\#}P < 0.05$, significantly different from the results in APB5-treated mice.

retinas almost completely rescued its vascular defects and BRB breakdown (Supplemental Figure 3, A–C). Therefore, we examined the effects of a CXCR4 block on mRNA expression of macrophage chemoattractant and adhesion molecules in APB5-treated retinas. As shown in Figure 5, APB5 treatment increased mRNA expression of macrophage chemoattractants CCL2 and CCL7 in mouse retinas but not CCL12 or CCL20 (Figure 5A). APB5 treatment also increased the expression of endothelial adhesion molecules ICAM-1, VCAM-1, and E selectin (Figure 5B). Pretreatment with AMD3100 significantly attenuated the increase in mRNA levels of CCL2, ICAM-1, and E selectin (Figure 5). CXCR4 inhibition may attenuate the infiltration of macrophages, at least partially, through these molecules.

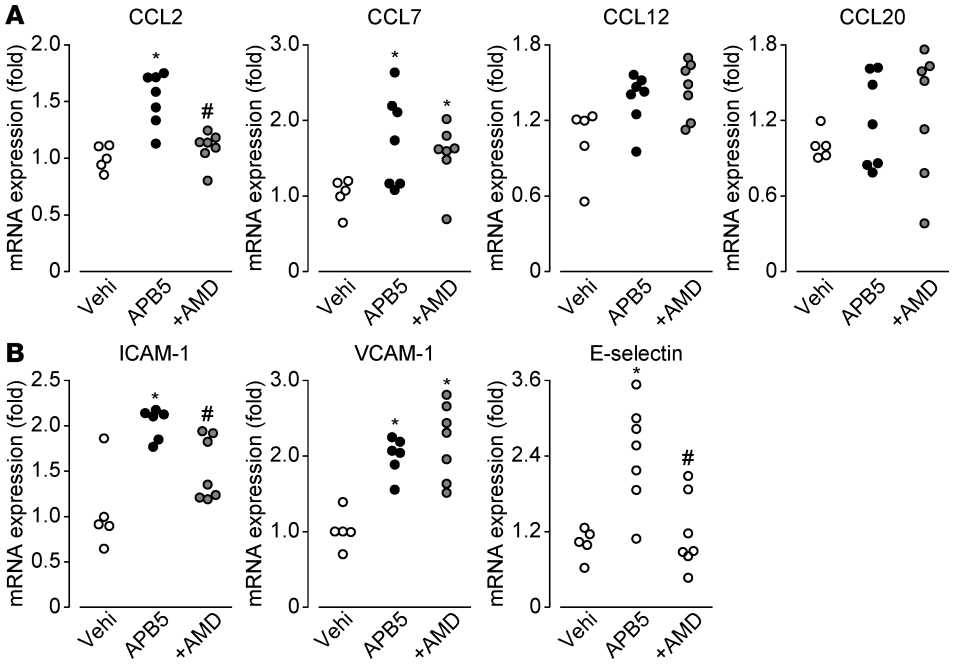

Figure 5. Endothelial CXCR4 increased the expression of chemoattractant and adhesion molecule. (**A**) The effect of APB5 or APB5 and AMD3100 (AMD) on macrophage chemoattractant mRNA expressions in P8 mouse retina (n = 8). (**B**) The effect of APB5 or APB5 and AMD3100 (AMD) on endothelial adhesion molecule mRNA expression in P8 mouse retina (n = 8). Significantly different from the results in vehicle-treated mice at $^{*}P < 0.05$, significantly different from the results in vehicle-treated mice. $^{\#}P < 0.05$, significantly different from the results in APB treated mice).

Discussion

SDF-1α is immediately upregulated under hypoxic conditions through the transcription factor hypoxia-inducible factor–1α (HIF-1α) (21). Previous reports show that HIF-1α–dependent SDF-1α upregulation occurs in astrocytes and/or ECs in several diseases, such as stroke and multiple sclerosis (22). Pericyte depletion induced by a PDGFRβ block is likely to decrease the number of perfused functional vessels and to cause hypoxia (20). This consequently induces SDF-1α expression, primarily in retinal ECs (Figure 1B).

We previously reported that APB5-induced pericyte depletion results in macrophage infiltration into perivascular areas that express VEGF, placental growth factor, and TNF-α (20). This phenomenon leads to sustained inflammation and subsequent BRB breakdown (20). Other groups have shown that, in streptozotocin-induced hyperglycemia, macrophages infiltrating the retina produce TNF-α, leading to vascular disruption and hyperpermeability (23, 24). Therefore, infiltrating macrophages play an important role in the progression of retinopathy.

Our current findings demonstrate that the endothelial-derived SDF-1α stimulated its receptor CXCR4, predominantly on ECs, and indirectly stimulated macrophage infiltration by inducing chemokine/adhesion molecule expression. Thus, SDF-1α may be a novel exacerbating factor that stimulates a vessel-damaging cycle between ECs and macrophages in retinopathy. SDF-1α might also have direct effect on ECs. We previously showed that SDF-1α/CXCR4 signal activation attenuated vascular permeability in croton oil–induced skin inflammation in mice ear (14). In contrast, other researchers showed the exacerbation of dipeptidyl peptidase 4 induced vascular leakage in mice ear (25). Further study is required to reveal its direct effect on ECs in progression of retinopathy.

Pharmacological block of CXCR4 decreased the expression of the macrophage chemoattractant CCL2 and endothelial adhesion molecules ICAM-1 and E selectin. CXCR4 is a Gi-type G protein–coupled receptor (26). There are several reports showing that the activation of Gi receptors increases the expression of these molecules in human and murine ECs via activation of p38 MAPK, JNK, and NF-κB signaling pathways (27–29). These pathways may be involved in the SDF-1α/CXCR4-induced expression of chemoattractant and adhesion molecules.

Anti-VEGF antibody has been widely used to treat DME (4). However, this therapy has several disadvantages in terms of disease unresponsiveness and adverse effects, including degeneration of choroidal vessels and macular atrophy (30–33). In our pericyte-deficient model, SDF-1α expression levels were elevated

as early as at P6, whereas macrophage infiltration increased at P6 (20). Thus, it seems likely that EC-derived SDF-1α initiates macrophage infiltration and amplifies the inflammatory loop between macrophages and ECs in the absence of pericytes. Blocking the SDF-1α signal may be a beneficial alternative strategy for DR patients who have lost responsiveness to anti-VEGF therapy (34).

In the present study, we identified SDF-1α/CXCR4 signaling as an exacerbating factor in the pericyte depletion–induced BRB breakdown and suggest therapeutic potential through its inhibition. Since administration of an anti-PDGFRβ antibody APB5 induced features characteristic of human DR, we believe that this model may mimic sequential events following pericyte dropout in human DR and prove useful in the assessment of therapeutic targets. It should be noted that we utilized postnatal retina angiogenesis, while human DR typically occurs at a relatively old age. Further studies are needed to evaluate the contribution and potential therapeutic application of SDF-1α/CXCR4 signaling in human DR.

Methods

Mice. Wild-type C57BL/6 mice were purchased from Sankyo Labo Service and Japan SLC. Pdgfb-iCreER^{T2} mice (35) were crossed with CXCR4$^{flox/flox}$ mice (36) to produce Pdgfb-iCreER^{T2}/CXCR4$^{flox/flox}$ mice. Littermates lacking the Pdgfb-iCreER^{T2} transgene (CXCR4$^{flox/flox}$) were used as controls. Conditional endothelial *Cxcr4* gene deficiency (CXCR4$^{i\Delta EC}$) was induced by intraperitoneal daily injection of 150 μg 4-hydroxytamoxifen (MilliporeSigma) in 50 μl peanut oil from P1 to P3.

Pericyte deficiency–induced BRB breakdown model. Rat anti-mouse PDGFRβ monoclonal antibody APB5 (18) was intraperitoneally injected into P1 mice (40 μg in 40 μl PBS). CXCR4 inhibitor AMD3100 (Abcam) at 40 mg/kg or FC131 (37) at 30 mg/kg was intraperitoneally injected at P3, P5, and P7. The retinas were analyzed at P8. In other experiments, AMD3100 was injected intraperitoneally daily from P8 through P10, and the retinas were analyzed at P11. For localized treatment, 1 μg AMD3100 in 0.6 μl PBS and/or 2.5 μg VEGF Trap (aflibercept, Bayer Pharma) in 0.6 μl PBS were intravitreally injected at P5, and the retinas were analyzed at P8. Clodronate liposomes (7 mg/ml in 50 ul PBS, i.p., P4 and P5) were injected to deplete infiltrating macrophages in mouse retinas. In all procedures, mock-treated littermate controls received injections of vehicle only. The severity of retinal edema and hemorrhage was graded at P11, as described previously (20). In brief, scores were defined as follows: grade 1, no hemorrhage and edema; grade 2, local hemorrhage and/or mild edema; grade 3, edema in up to one half of the retina; and grade 4, collapse of the retina.

Morphological analysis. Following fixation of P8 mouse eyes with 4% paraformaldehyde (PFA) in PBS for 20 minutes, the retinal cups were dissected and further fixed in 4% PFA in PBS for 10 minutes. The fixed retinas were blocked with 1% bovine serum albumin and 0.5% Triton X-100 in PBS for 2 hours and then incubated overnight with primary antibody rabbit anti-mouse desmin (Abcam; 1:200), rabbit anti-human fibrinogen (Dako; 1:500), or rat anti-mouse F4/80 (Bio-Rad, Tokyo; 1:200). The retinas were then treated with Alexa Fluor 594–conjugated isolectin B_4 (Thermo Fisher Scientific; 1:200) and either secondary antibody Alexa Fluor 488 anti-rabbit antibody (Thermo Fisher Scientific; 1:500) or secondary antibody Alexa Fluor 488 anti-rat antibody (Thermo Fisher Scientific; 1:500), as appropriate, for 2 hours in 1 mM $CaCl_2$, 1 mM $MgCl_2$, 1 mM $MnCl_2$, and 1% Triton X-100 in PBS. Nuclei were labeled with DAPI (MilliporeSigma) at 1 μg/ml for 15 minutes. Fluorescent and confocal microscopic images were captured using a Nikon Eclipse Ti microscope and C1 confocal system (Nikon). The images were analyzed with NIS-Elements D software (Nikon). The radii of retinal vascular networks were calculated using the distances from the optic nerve to the angiogenic front. The vessel diameters were calculated by averaging those for 3 arteries and veins per retina, approximately 200–300 μm from the optic nerve head. Fibrinogen intensity was calculated measuring 20 random areas at the vascular front per retina. The number of macrophages per area was estimated from counts in four 300 × 300–μm fields per retina.

Real-time PCR. Retinas were harvested at P5, P7, P8, and P9 from mice treated by intraperitoneal injection of 40–60 μg APB5 in 40 μl PBS or were mock treated with vehicle only at P1. Total RNA was extracted using TRI-Reagent (Molecular Research Center, Cincinnati, Ohio, USA) and the first strand of cDNA was reverse transcribed using a random 9-mer primer (TOYOBO) and ReverTra Ace (TOYOBO), as directed by the manufacturers. The cDNA was amplified using Platinum SYBR Green qPCR SuperMix-UDG (Thermo Fisher Scientific) and AriaMx Real-Time PCR System (Agilent Technologies). The mRNA expression levels were quantitated with the ΔCt method, using 18S rRNA or TBP mRNA levels as endogenous controls. Primer sequences are shown in Supplemental Table 1.

In situ hybridization. *Sdf1a* and *Cxcr4* mRNA expression in whole-mount retinas was detected using digoxigenin-labeled (DIG-labeled) cRNA probes and alkaline phosphatase–conjugated (AP-conjugated) anti-DIG antibody (Roche) followed by NBT/BCIP staining (Roche), as previously described (38). After in situ hybridization, the retinas were immunostained with rabbit anti-type IV collagen antibody (Cosmo Bio) and biotinylated by anti-rabbit antibody (VECTOR). The AP and DAB staining was assessed with an OPTIHOT-2 microscope (Nikon) equipped with associated software (ACT-1C, Nikon).

Flow cytometry. Flow cytometry was conducted as previously described (39–41). P8 retinas were mechanically dissociated and enzymatically digested using 0.5 mg/ml collagenase D (MilliporeSigma) and 750 U/ml DNase (MilliporeSigma) in Hanks' balanced salt solution (MilliporeSigma) for 25 minutes. Retinas were then forced through a 100-μm nylon mesh to obtain single-cell suspensions. Cells were labeled with fluorescence-conjugated antibodies for 30 minutes as follows: Alexa Fluor 488 anti-mouse CD45 (Biolegend), PE anti-mouse/human CD11b (Biolegend), PE anti-mouse CD31 (Biolegend), or Alexa Fluor 647 anti-mouse CD184 (CXCR4). Viability staining solution 7-aminoactinomycin D (7-AAD; Biolegend) was applied for 5 minutes, and the analyses were conducted using a BD Accuri C6 Flow Cytometer (BD Biosciences). Following removal of dead cells based on 7-AAD labeling, the doublet cells were excluded using forward scatter height (FSC-H) versus forward scatter width (FSC-W) gates. Further analyses were conducted using BD Accuri C6 Software (BD Biosciences).

Statistics. Data are shown as mean ± SEM. Statistical evaluation between 2 groups was conducted by Student's *t* test (2 tailed, parametric) or Mann-Whitney's *U* test (nonparametric). Statistical evaluation of 3 groups was performed by 1-way ANOVA followed by Tukey's test. A value of $P < 0.05$ was considered to indicate statistically significant differences.

Study approval. Animal experiments were approved by the Institutional Animal Care and Use Committee of The University of Tokyo and the Animal Research Committee of Nagoya City University and performed according to the Association for Research in Vision and Ophthalmology Statement for the Use of Animals in Ophthalmic and Vision Research.

Author contributions

KO conducted experiments, acquired and provided data, and wrote the manuscript. KK, YF, NN, and ES conducted experiments and acquired and provided data. NF, TNH, YT, MF, and TN analyzed data and provided reagents. AU designed research studies, analyzed data, provided reagents, and wrote the manuscript. TM designed research studies, analyzed data, and wrote the manuscript.

Acknowledgments

This work was supported by a Grant-in-Aid for Japan Society for the Promotion of Science fellows (no. 10795) to KO and by a Grant-in-Aid from the Japan Society for the Promotion of Science (17H01509 and 17H06252), the Charitable Trust Fund for Ophthalmic Research in Commemoration of Santen Pharmaceutical's Founder, the SENSHIN Medical Research Foundation, the Cardiovascular Research Fund, the Nakatomi Foundation, the Naito Foundation (to TM), and the NOVARTIS Foundation (Japan) for the Promotion of Science.

Address correspondence to: Takahisa Murata, 1-1-1, Yayoi, Bunkyo-ku, Tokyo 113-8657, Japan. Phone: 81.3.5841.7247; Email: amurata@mail.ecc.u-tokyo.ac.jp.

1. Yau JW, et al. Global prevalence and major risk factors of diabetic retinopathy. *Diabetes Care*. 2012;35(3):556–564.
2. Antonetti DA, Klein R, Gardner TW. Diabetic retinopathy. *N Engl J Med*. 2012;366(13):1227–1239.
3. Aiello LP, et al. Vascular endothelial growth factor in ocular fluid of patients with diabetic retinopathy and other retinal disorders. *N Engl J Med*. 1994;331(22):1480–1487.
4. Diabetic Retinopathy Clinical Research Network, et al. Aflibercept, bevacizumab, or ranibizumab for diabetic macular edema. *N Engl J Med*. 2015;372(13):1193–1203.
5. Arevalo JF, et al. Primary intravitreal bevacizumab for diffuse diabetic macular edema: the Pan-American Collaborative Retina Study Group at 24 months. *Ophthalmology*. 2009;116(8):1488–1497.e1.
6. Bromberg-White JL, Glazer L, Downer R, Furge K, Boguslawski E, Duesbery NS. Identification of VEGF-independent cytokines in proliferative diabetic retinopathy vitreous. *Invest Ophthalmol Vis Sci*. 2013;54(10):6472–6480.
7. Dai Y, Wu Z, Wang F, Zhang Z, Yu M. Identification of chemokines and growth factors in proliferative diabetic retinopathy vitreous. *Biomed Res Int*. 2014;2014:486386.
8. Brooks HL, et al. Vitreous levels of vascular endothelial growth factor and stromal-derived factor 1 in patients with dia-

betic retinopathy and cystoid macular edema before and after intraocular injection of triamcinolone. *Arch Ophthalmol*. 2004;122(12):1801–1807.
9. Chatterjee M, et al. Platelet-derived CXCL12 regulates monocyte function, survival, differentiation into macrophages and foam cells through differential involvement of CXCR4-CXCR7. *Cell Death Dis*. 2015;6:e1989.
10. Petit I, et al. G-CSF induces stem cell mobilization by decreasing bone marrow SDF-1 and up-regulating CXCR4. *Nat Immunol*. 2002;3(7):687–694.
11. Pi X, Wu Y, Ferguson JE, Portbury AL, Patterson C. SDF-1alpha stimulates JNK3 activity via eNOS-dependent nitrosylation of MKP7 to enhance endothelial migration. *Proc Natl Acad Sci USA*. 2009;106(14):5675–5680.
12. Itoh T, et al. The relationship between SDF-1alpha/CXCR4 and neural stem cells appearing in damaged area after traumatic brain injury in rats. *Neurol Res*. 2009;31(1):90–102.
13. Strasser GA, Kaminker JS, Tessier-Lavigne M. Microarray analysis of retinal endothelial tip cells identifies CXCR4 as a mediator of tip cell morphology and branching. *Blood*. 2010;115(24):5102–5110.
14. Kobayashi K, et al. Stromal cell-derived factor-1α/C-X-C chemokine receptor type 4 axis promotes endothelial cell barrier integrity via phosphoinositide 3-kinase and Rac1 activation. *Arterioscler Thromb Vasc Biol*. 2014;34(8):1716–1722.
15. Cogan DG, Toussaint D, Kuwabara T. Retinal vascular patterns. IV. Diabetic retinopathy. *Arch Ophthalmol*. 1961;66:366–378.
16. Klinghoffer RA, Mueting-Nelsen PF, Faerman A, Shani M, Soriano P. The two PDGF receptors maintain conserved signaling in vivo despite divergent embryological functions. *Mol Cell*. 2001;7(2):343–354.
17. Enge M, et al. Endothelium-specific platelet-derived growth factor-B ablation mimics diabetic retinopathy. *EMBO J*. 2002;21(16):4307–4316.
18. Uemura A, et al. Recombinant angiopoietin-1 restores higher-order architecture of growing blood vessels in mice in the absence of mural cells. *J Clin Invest*. 2002;110(11):1619–1628.
19. Lindblom P, et al. Endothelial PDGF-B retention is required for proper investment of pericytes in the microvessel wall. *Genes Dev*. 2003;17(15):1835–1840.
20. Ogura S, et al. Sustained inflammation after pericyte depletion induces irreversible blood-retina barrier breakdown. *JCI Insight*. 2017;2(3):e90905.
21. Ceradini DJ, et al. Progenitor cell trafficking is regulated by hypoxic gradients through HIF-1 induction of SDF-1. *Nat Med*. 2004;10(8):858–864.
22. Li M, Ransohoff RM. Multiple roles of chemokine CXCL12 in the central nervous system: a migration from immunology to neurobiology. *Prog Neurobiol*. 2008;84(2):116–131.
23. Portillo JC, et al. CD40 in retinal Müller cells induces P2X7-dependent cytokine expression in macrophages/microglia in diabetic mice and development of early experimental diabetic retinopathy. *Diabetes*. 2017;66(2):483–493.
24. Rangasamy S, McGuire PG, Franco Nitta C, Monickaraj F, Oruganti SR, Das A. Chemokine mediated monocyte trafficking into the retina: role of inflammation in alteration of the blood-retinal barrier in diabetic retinopathy. *PLoS One*. 2014;9(10):e108508.
25. Lee CS, et al. Dipeptidyl peptidase-4 inhibitor increases vascular leakage in retina through VE-cadherin phosphorylation. *Sci Rep*. 2016;6:29393.
26. Murphy PM, et al. International union of pharmacology. XXII. Nomenclature for chemokine receptors. *Pharmacol Rev*. 2000;52(1):145–176.
27. Lee HY, et al. Sphingosylphosphorylcholine stimulates CCL2 production from human umbilical vein endothelial cells. *J Immunol*. 2011;186(7):4347–4353.
28. Dzenko KA, Song L, Ge S, Kuziel WA, Pachter JS. CCR2 expression by brain microvascular endothelial cells is critical for macrophage transendothelial migration in response to CCL2. *Microvasc Res*. 2005;70(1-2):53–64.
29. Herlaar E, Brown Z. p38 MAPK signalling cascades in inflammatory disease. *Mol Med Today*. 1999;5(10):439–447.
30. Simó R, Hernández C. Novel approaches for treating diabetic retinopathy based on recent pathogenic evidence. *Prog Retin Eye Res*. 2015;48:160–180.
31. Ford JA, Lois N, Royle P, Clar C, Shyangdan D, Waugh N. Current treatments in diabetic macular oedema: systematic review and meta-analysis. *BMJ Open*. 2013;3(3):e002269.
32. Bolinger MT, Antonetti DA. Moving Past Anti-VEGF: Novel Therapies for Treating Diabetic Retinopathy. *Int J Mol Sci*. 2016;17(9):1498.
33. Ehrlich R, Dan I, Deitch I, Axer-Siegel R, Mimouni K. The effectiveness of intravitreal ranibizumab in patients with diabetic macular edema who have failed to respond to intravitreal bevacizumab. *Ophthalmologica*. 2016;235(3):133–136.
34. Yang CS, Hung KC, Huang YM, Hsu WM. Intravitreal bevacizumab (Avastin) and panretinal photocoagulation in the treatment of high-risk proliferative diabetic retinopathy. *J Ocul Pharmacol Ther*. 2013;29(6):550–555.
35. Claxton S, Kostourou V, Jadeja S, Chambon P, Hodivala-Dilke K, Fruttiger M. Efficient, inducible Cre-recombinase activation in vascular endothelium. *Genesis*. 2008;46(2):74–80.
36. Tokoyoda K, Egawa T, Sugiyama T, Choi BI, Nagasawa T. Cellular niches controlling B lymphocyte behavior within bone marrow during development. *Immunity*. 2004;20(6):707–718.
37. Fujii N, et al. Molecular-size reduction of a potent CXCR4-chemokine antagonist using orthogonal combination of conformation- and sequence-based libraries. *Angew Chem Int Ed Engl*. 2003;42(28):3251–3253.
38. Uemura A, Kusuhara S, Wiegand SJ, Yu RT, Nishikawa S. Tlx acts as a proangiogenic switch by regulating extracellular assembly of fibronectin matrices in retinal astrocytes. *J Clin Invest*. 2006;116(2):369–377.
39. Dejda A, et al. Neuropilin-1 mediates myeloid cell chemoattraction and influences retinal neuroimmune crosstalk. *J Clin Invest*. 2014;124(11):4807–4822.
40. Kerr EC, Raveney BJ, Copland DA, Dick AD, Nicholson LB. Analysis of retinal cellular infiltrate in experimental autoimmune uveoretinitis reveals multiple regulatory cell populations. *J Autoimmun*. 2008;31(4):354–361.
41. Kusuhara S, et al. Arhgef15 promotes retinal angiogenesis by mediating VEGF-induced Cdc42 activation and potentiating RhoJ inactivation in endothelial cells. *PLoS One*. 2012;7(9):e45858.